ASEAN Engineering Journal

Full Paper

INFLUENCE OF SURFACE METEOROLOGICAL DATA ON AERMOD-SIMULATED TSP DISPERSION FROM MDF FACTORY

Pathanin Kiniman, Thaniya Kaosol*

Department of Civil and Environmental Engineering, Faculty of Engineering, Prince of Songkla University, Hat Yai, 90110 Songkhla, Thailand

Article history
Received
01 October 2025
Received in revised form
25 January 2026
Accepted
01 April 2026
Published online
31 August 2026

*Corresponding author
thaniya.k@psu.ac.th

Graphical abstract

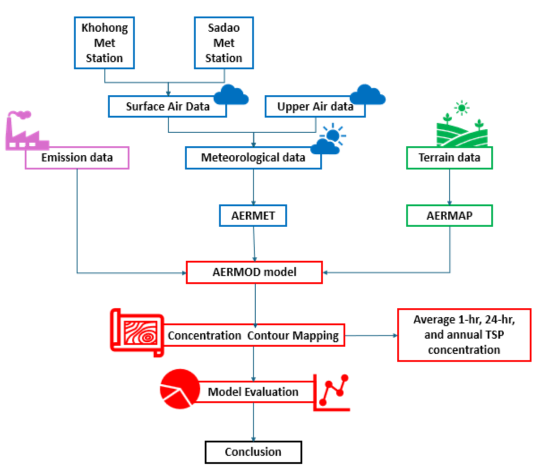

Abstract

This study evaluates the influence of surface meteorological data on the dispersion of Total Suspended Particulates (TSP) emitted from a Medium Density Fiberboard (MDF) factory in Southern Thailand using AERMOD model. Meteorological inputs from two nearby stations, Khohong and Sadao, were applied to simulate emissions from six stacks and predict concentrations at 15 receptors within a 10 km radius during 2020–2023. The results demonstrated that Sadao data generated higher localized concentrations due to weaker winds and more stable atmospheric conditions, whereas Khohong data produced wider dispersion plumes with lower ground-level concentrations under stronger mixing. Despite these differences, all predicted values complied with Thailand's National Ambient Air Quality Standards (NAAQS) (24-hour: 200 µg/m^3; annual: 80 µg/m^3). Model validation indicated moderate agreement with observations, highlighting both the capability of AERMOD for regulatory applications and the sensitivity of outcomes to meteorological inputs. The findings underscore the importance of selecting appropriate meteorological stations in tropical monsoon climates to ensure accurate and representative air quality assessments.

Keywords: AERMOD, Fiber dust, TSP, MDF, Meteorological data

1.0 INTRODUCTION

The Medium Density Fiberboard (MDF) industry represents a cornerstone of Thailand's wood-processing and furniture manufacturing sectors, particularly in the southern provinces where rubberwood serves as the primary raw material. Economically significant, this industry simultaneously poses notable environmental and occupational health challenges. MDF is a composite wood product manufactured by breaking down hardwood or softwood residuals into lignocellulosic fibers, which are subsequently bonded with synthetic resins, typically urea-formaldehyde (UF). The UF content in MDF generally ranges between 8-18% [1]. Under conditions of high temperature and pressure, resin-coated fibers are compressed into dense, uniform panels valued for their smooth surface, workability, and absence of natural wood defects, making MDF an important material in furniture, cabinetry, and interior fittings [2]-[5].

Despite its widespread utility, MDF production and subsequent machining generate considerable airborne dust, primarily classified as Total Suspended Particulates (TSP). This dust, consisting of fine wood fibers and cured resins, presents significant occupational health risks [6]. The physical characteristics of dust are influenced by operational parameters such as cutting speed, with high-speed milling producing finer, more respirable particles [3][7]. Prolonged exposure to MDF dust and formaldehyde emissions has been linked to respiratory problems, contact dermatitis, and musculoskeletal disorders [8][9]. Regulatory agencies, including the Occupational Safety and Health Administration (OSHA), recognize wood dust as a workplace hazard and have established occupational exposure limits [10].

From an environmental perspective, uncontrolled TSP emissions from MDF factories contribute to local air quality degradation, posing risks to nearby communities and ecosystems [11]. Although Thailand enforces air quality standards, such as the National Ambient Air Quality Standards (NAAQS), accurately assessing the direct impact of specific industrial sources remains challenging [12]. In this context, dispersion models are essential tools for evaluating pollutant transport and exposure risks. The AERMOD (AMS/EPA Regulatory Model) is widely recognized as a state-of-the-science dispersion model that incorporates advanced planetary boundary layer physics and is extensively validated for regulatory applications [13]-[18].

The application of AERMOD has been documented in diverse industrial and geographical contexts, including cement plants and complex industrial zones [19]-[23]. Its accuracy, however, depends strongly on the quality of meteorological input. Studies indicate that model performance varies under different stability regimes and can be enhanced when coupled with prognostic weather models such as the Weather Research and Forecasting (WRF) model [24]-[26]. AERMOD has further been applied to air quality assessments in Thailand, for example, to evaluate NO_2 and SO_2 dispersion in industrial complexes such as Map Ta Phut [27][28].

This study applies AERMOD to simulate the dispersion of TSP emissions from MDF factory in Songkhla Province, Southern Thailand. To capture the influence of the region's distinct monsoon climate [29][30], the model incorporates both surface and upper-air meteorological data from two synoptic weather stations, using formats compatible with global archives such as the Integrated Global Radiosonde Archive (IGRA) [31]. By conducting comparative analysis of different meteorological datasets, the study evaluates the sensitivity of dispersion outcomes to local weather inputs, an approach that has been emphasized in prior research [32].

Although air quality modeling has been conducted in Thailand, research focusing specifically on TSP emissions from MDF manufacturing using localized meteorological data remains limited. Local community concerns regarding elevated dust levels highlight the urgent need for site-specific, evidence-based assessments. Accordingly, this study seeks to address this gap by applying AERMOD to quantify TSP emissions, assess the influence of meteorological inputs from different stations, and compare predicted concentrations with Thailand's NAAQS. The outcomes aim to provide a robust basis for regulatory planning, health risk assessment, and policy development in managing particulate pollution from industrial sources.

2.0 METHODOLOGY

2.1 Study Area

The study area is an MDF factory located in Patong Subdistrict, Hat Yai District, Songkhla Province, Southern Thailand (Figure 1). Patong lies approximately 28 km southeast of Hat Yai city and covers a land area of 126.16 km^2, making it one of the larger and more economically significant subdistricts in the region. Administratively, the study area is located within Hat Yai District, the largest and most economically influential district in Southern Thailand, with a permanent population of over 400,000 and a substantial floating population.

Geographically, Patong Subdistrict is bordered by Ban Pru and Thung Lan to the north, Phang La and Khao Mee Kiat to the south, Kae and Na Khao to the east, and Thung Lan of Khlong Hoi Khong District to the west. It is situated between 6°55′-6°58′ N latitude and 100°28′-100°31′ E longitude, placing it within the lower southern peninsula of Thailand. Its location midway between the Gulf of Thailand and the inland mountain ranges exposes it to both orographic rainfall and coastal weather dynamics, which are critical factors influencing local meteorology and, consequently, air quality modeling.

Topographically, the subdistrict comprises a mix of flat plains and rolling hills, with elevations ranging from 20 to 150 m above mean sea level. The northern zone is predominantly flat and utilized for agriculture and settlement, whereas the southern zone is characterized by more undulating terrain. These variations influence land use, hydrology, and microclimatic conditions, making topography an important determinant in dispersion modeling. This physical landscape exerts a direct influence on land-use patterns. The southern zone is characterized by undulating terrain predominantly occupied by para rubber plantations, whereas the northern and central zones have experienced rapid urbanization. In this study, the classification of these areas as urban for land-use parameterization is justified by the high density of built-up areas, commercial establishments, and concentrated residential developments within Patong Subdistrict, particularly along the industrial corridor. These characteristics are indicative of the broader urban expansion of the Hat Yai metropolitan area.

Climatically, Patong experiences a tropical monsoon climate typical of Southern Thailand [33]. The southwest monsoon (May-October) and the northeast monsoon (November-January) bring heavy rainfall and persistent humidity, separated by short inter-monsoon periods with highly variable wind directions. Such seasonal dynamics affect wind speed, wind direction, and atmospheric stability, which are vital parameters for predicting the dispersion of TSP from industrial sources such as the MDF factory.

Given its unique combination of geography, climate, population, and industrial infrastructure, Patong represents a particularly suitable case study for assessing the environmental impacts of industrial emissions using models such as AERMOD. The presence of major transportation corridors and cross-border economic activities further underscores the need for integrated land-use planning and sustainable air quality management in this region.

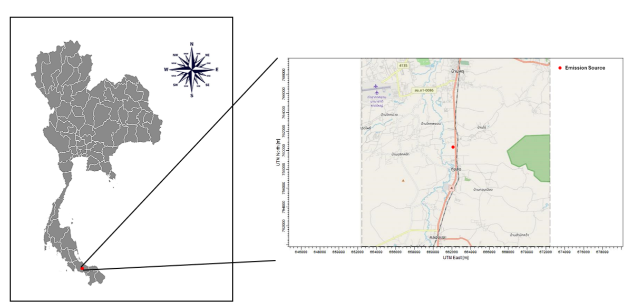

Figure 1 Study area

2.2 Data And Procedure

2.2.1 Collecting Required Information For Model Input

2.2.1.1 Emission Sources

The TSP emissions from the factory were estimated for six stacks over the study period from 2020 to 2023. These estimates served as primary inputs for the dispersion modeling. For the example of emission sources data on 2020 as shown on Table 1

Table 1 Emission sources on 2020

Stack ID	Stack name	UTM coordinate		Stack height	Stack inner diameter	Stack temperature	Stack velocity	TSP emission rate
		X	Y	(m)	(m)	(K)	(m/s)	(g/s)
STCK1	DRYER1_MDF1	661815	759760	50	3.0	333.20	34.30	2.803
STCK2	DRYER2_MDF1	661824	759783	50	3.0	335.85	20.55	2.388
STCK3	ESP_MDF1	661784	759919	40	2.3	585.00	6.87	1.585
STCK4	DRYER1_MDF2	661579	760406	50	3.5	333.13	24.90	12.080
STCK5	DRYER2_MDF2	661589	760394	50	3.5	330.50	24.90	10.584
STCK6	ESP_MDF2	661687	760423	40	2.5	577.00	11.70	0.713

2.2.1.2 Receptor Points

Receptor locations were established within 5 and 10 km radius from the center of emission sources, as summarized in Table 2. Two receptor types were considered: (i) grid receptors, representing risk receptors generated using the AERMAP preprocessor, and (ii) sensitive receptors, represented by discrete cartesian receptor points. Information recorded for each receptor included receptor ID, geographic coordinates in UTM (X,Y), receptor grouping, and elevation above mean sea level (MSL). The spatial distribution of all receptors is presented in Figure 2.

Figure 2 Receptors

2.2.1.3 Meteorological Data

For this study, the surface meteorological data was obtained from two stations located near the emission source: Khohong Meteorological Station and Sadao Meteorological Station. These stations differ in elevation, station type, measurement height, and program affiliations, as summarized in Table 3. The comparative use of these datasets allowed for the assessment of how station-specific characteristics influence dispersion modeling outcomes.

The original datasets were recorded as three-hour synoptic observations. For input into the AERMOD dispersion model, the data were processed and converted into hourly records to ensure compatibility with model requirements and to provide sufficient temporal resolution for simulating pollutant dispersion dynamics.

Table 2 Sensitive receptors (Discrete cartesian receptors)

Receptor ID	Group of receptors	UTM coordinate		Height from MSL (m)
		X (m)	Y (m)	
R1	MUNICIPALITY	661905.00	759429.00	24.50
R2	VILLAGE	662401.00	760267.00	19.21
R3	VILLAGE	661513.00	760765.00	20.24
R4	MOSQUE	664306.17	761592.60	23.27
R5	SCHOOL	661925.28	761323.59	21.37
R6	VILLAGE	661495.59	760801.69	18.15
R7	VILLAGE	661267.53	764427.28	12.07
R8	VILLAGE	662434.44	760336.29	22.22
R9	POLICE STATION	662903.01	759700.12	30.11
R10	HOSPITAL	657879.44	759804.48	25.00
R11	MUNICIPALITY	658621.67	760549.14	15.13
R12	TEMPLE	658510.72	760832.32	18.41
R13	VILLAGE	661161.34	759040.82	19.11
R14	TEMPLE	662466.07	757727.16	20.00
R15	HOSPITAL	662433.67	757456.02	21.00

Table 3 Meteorological station data

Parameter	Khohong (48571)	Sadao (48574)
Coordinates	7.0156°N,100.5017°E	6.7872°N, 100.4128°E
Elevation (m)	6.96	24.7
Station type	GBON, Surface land SYNOP	GBON, Hydrological, Surface land SYNOP
Programs/affiliations	GBON, GOS General	GBON, RBON, GOS General, Hydromet
Reporting interval	3 hr	3 hr
Measurements reported	Cloud amount, base, type; RH; temp; pressure; wind speed/direction; visibility; soil temp; evaporation; sunshine duration	Cloud amount, base, type; RH; temp; pressure; wind speed/direction; visibility; evaporation; hydrology (stream discharge and level)
Wind measurement height	16.96 m	34.7 m
Supervising organization	Thai Meteorological Department	Thai Meteorological Department
Special features	Includes soil temperature data	Includes hydrological measurements (stream discharge and level)
Distance from emission sources	17 km	27 km

2.2.2 AERMOD Model

AERMOD (American Meteorological Society/Environmental Protection Agency Regulatory Model) is one of the most widely applied and scientifically validated air dispersion models for regulatory and environmental assessments. Developed jointly by the American Meteorological Society (AMS) and the U.S. EPA through the AERMIC (AMS/EPA Regulatory Model Improvement Committee), AERMOD was formally designated in 2005 as the EPA's preferred regulatory model, replacing the ISCST3 model [13][14][16]. It is specifically designed to simulate pollutant dispersion from industrial and stationary sources over distances up to 50 km.

In Thailand, the Office of Natural Resources and Environmental Policy and Planning (ONEP) approved the use of AERMOD for Environmental Impact Assessments (EIA) in 2007. Since then, it has been extensively employed in EIAs for industrial projects, particularly for regulatory compliance in air quality assessments. Its adoption is further supported by academic studies validating its suitability under local meteorological and topographic conditions. Chusi et al. [28] demonstrated AERMOD's capability for near-field dispersion modeling in Thailand. National endorsement of the model ensures consistency, precision, and scientific rigor in environmental evaluations [35].

AERMOD is a steady-state Gaussian plume model that incorporates advanced Planetary Boundary Layer (PBL) physics. It accounts for atmospheric turbulence, surface friction, and vertical mixing using surface-layer and mixed-layer scaling approaches, dynamically adjusting dispersion according to atmospheric stability conditions. Under stable nocturnal conditions, pollutant dispersion follows a Gaussian distribution in both horizontal and vertical dimensions. Under convective daytime conditions, the model applies a Gaussian distribution horizontally and a bi-Gaussian probability density function vertically [23].

Meteorological and terrain inputs are processed using two pre-processors: AERMET, which handles surface and upper-air meteorological data such as wind speed, wind direction, temperature, and atmospheric stability; and AERMAP, which processes terrain data for simple and complex topographies [16]. To enhance the accuracy of vertical profiles, upper-air data from the Integrated Global Radiosonde Archive (IGRA) were employed in this study. IGRA provides globally consistent, quality-controlled profiles of temperature, wind, and pressure, supporting reliable estimation of mixing heights and stability classes [32].

Numerous validation studies have confirmed AERMOD's predictive reliability. Reported accuracy ranges from 72-89% for 1-hour averages and 85-95% for annual mean concentrations when using high-quality input data [36]. The model has also been successfully applied to particulate matter studies in diverse national and international contexts. For instance, Kakosimos et al. [22] assessed its performance in simulating PM emissions from industrial sources in the Greater Thessaloniki area, confirming its robustness under complex meteorological regimes. In the context of TSP from MDF factories, AERMOD effectively incorporates parameters such as particle size distribution, gravitational settling, and deposition velocities, enabling refined estimates of downwind concentrations [27]. The overall structure of AERMOD modeling system, including data inputs and processing flow applied in this study, is illustrated in Figure 3. For this study, to analyze and simulate TSP dispersion using AERMOD View 13.0.0 (Serial# AER0012816) which has been developed by Lakes Environmental Software.

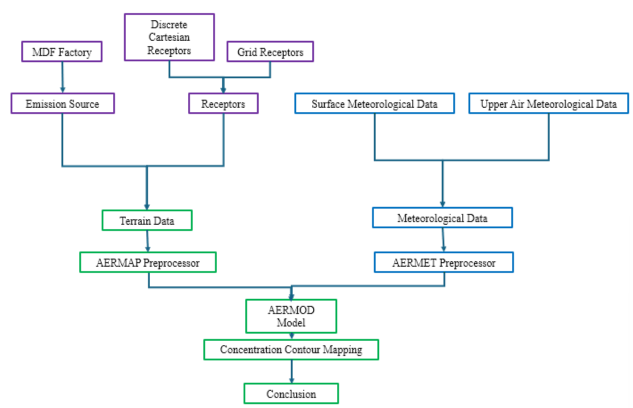

Figure 3 Diagram of AERMOD model

The AERMOD dispersion modeling system comprises three key components: the dispersion module (AERMOD), the meteorological pre-processor (AERMET), and the terrain pre-processor (AERMAP). The AERMET module requires land-use classifications (e.g., urban and non-urban) and parameters such as albedo, Bowen ratio, and surface roughness length. It also utilizes surface meteorological data including wind speed, wind direction, dry-bulb temperature, cloud cover, and ceiling heigh recorded at observation sites (Khohong Meteorological Station and Sadao Meteorological Station), together with upper-air meteorological data obtained from Songkhla Station in the IGRA format. Based on these inputs, AERMET calculates boundary-layer parameters required by AERMOD, including friction velocity, Monin–Obukhov length, convective velocity scale, temperature scale, mixing height, and surface heat flux.

The terrain pre-processor, AERMAP, assigns elevations to all receptors and emission sources in the modeling domain [37]. In this study, AERMOD version 13.0.0 was applied to assess the influence of meteorological data on the dispersion of TSP emitted from an MDF factory in Hat Yai District, Songkhla Province, Thailand. The analysis covered a four-year period, from 2020 to 2023, to evaluate annual and seasonal variability in model predictions.

2.2.3 Running AERMET Pre-Processor

AERMET is used to calculate the boundary-layer parameters required for AERMOD, based on input meteorological data and surface characteristics of the study area [38]. For this study, meteorological observations were obtained from two stations in Songkhla Province. The original datasets, provided in Excel format, were converted into SCRAM-compatible files prior to use in AERMET. Profile parameters considered included wind speed and direction, temperature, cloud cover, and ceiling height.

AERMET also requires three land-use parameters: Bowen ratio, albedo, and surface roughness length. These values were determined by dividing the study area into appropriate land-use and vegetation categories. Based on this classification, one segment was designated as an urban area, and the corresponding values of the three parameters were specified monthly. Seasonal conditions were further characterized according to the Southern Thailand monsoon regime, as summarized in Table 4.

In addition, AERMET incorporates upper-air data to improve vertical structure estimation. For this study, upper-air profiles in the IGRA format were used. IGRA provides globally consistent radiosonde and pilot balloon data, available from as early as 1905 [32]. The data used to cover the entire study period, with upper-air information derived primarily from Forecast Systems Laboratory (FSL) data and, in some cases, from Weather Research and Forecasting (WRF) model outputs.

Table 5 presents wind rose plots for the study region based on meteorological data from Khohong and Sadao stations during 2020-2023. The results reflect the dominant influence of Thailand's northeast and southwest monsoons, with prevailing winds primarily from the Northeast (NE) to Southwest (SW) sectors. Interannual variations in wind direction and intensity were evident, highlighting the influence of seasonal monsoon regimes and local meteorological conditions on wind behavior.

Table 4 The land use parameters of study area on monthly basis (seasonal/month selection)

Month	Albedo coefficient	Bowen ratio	Surface roughness length
January	0.16	2	1
February	0.16	2	1
March	0.16	2	1
April	0.16	2	1
May	0.14	1	1
June	0.14	1	1
July	0.14	1	1
August	0.14	1	1
September	0.14	1	1
October	0.14	1	1
November	0.14	1	1
December	0.14	1	1

While using Khohong meteorological station, wind directions during 2020 were predominantly from the NE and east (E) sectors, with most wind speed in the 2-4 m/s and 4-6 m/s ranges. Maximum speeds reached 8-10 m/s, while calm conditions (<2 m/s) represented a significant portion of the dataset, reflecting the influence of regional trade winds modulated by the urban–agricultural landscape. In 2021, prevailing winds remained similar, though the frequency of 4-6 m/s winds increased, with occasional peaks of 10-13 m/s, suggesting marginal intensification linked to synoptic-scale variability. In 2022, NE winds continued to dominate, with 2-4 m/s remaining the most frequent category and higher speeds (>8 m/s) occurring infrequently, consistent with stable atmospheric conditions and limited mixing. By 2023, a subtle shift towards East-Southeast (ESE) winds, was observed, accompanied by more frequent winds in the 4-6 m/s range, though maximum speeds above 10 m/s remained rare.

In contrast, Sadao recorded broader directional distributions and generally higher wind speeds. In 2020, winds were distributed across NE and SW quadrants, dominated by the 4-6 m/s and 6-8 m/s categories, with maximum speeds up to 16 m/s. This reflects stronger regional flows and reduced surface friction due to higher measurement heights. In 2021, similar NE dominance was observed with reduced SW contributions, and wind speeds frequently fell in the 2-6 m/s range, with occasional peaks up to 13 m/s, typical of transitional monsoon periods. In 2022, strong NE winds were accompanied by higher frequencies in the 6-10 m/s categories, indicating more robust transport conditions compared with Khohong. By 2023, winds again exhibited NE and SW components, with maximum speeds reaching 16 m/s, underscoring the station's capacity to capture high wind events critical for transboundary pollution modeling.

Overall, Sadao consistently measured higher maximum wind speeds (up to 16 m/s) and broader directional variability than Khohong. These differences can be attributed to anemometer height and surrounding terrain: Sadao elevated instruments and open landscape reduce surface roughness, enabling better representation of ambient flow patterns, while Khohong urban–agricultural interface introduces frictional drag that attenuates wind speeds and constrains directional variability. Operational context also plays a role; Sadao data are particularly suited for regional-scale dispersion and transboundary pollution studies, whereas Khohong data are more appropriate for localized assessments, agrometeorological studies, and urban microclimate analyses, including near-field particulate matter dispersion.

Table 5 Compare wind rose between Khohong and Sadao meteorological station

Year/Station	Khohong	Sadao
2020	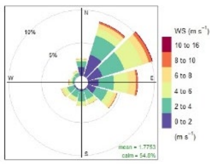	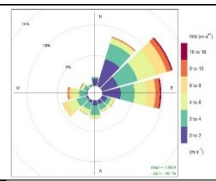
2021	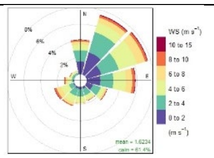	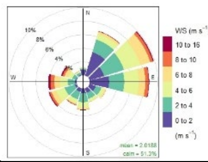
2022	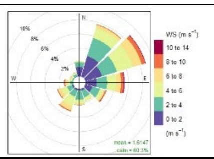	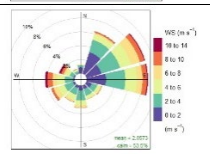
2023	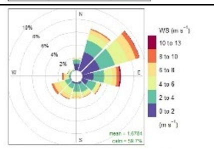	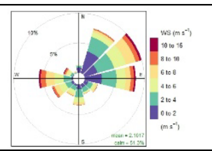

2.2.4 Running AERMAP Pre-Processor

AERMOD terrain preprocessor (AERMAP) serves as the terrain pre-processor within the AERMOD modeling system. It is employed to analyze the topographical characteristics of the study area and to assign elevations to all receptors and emission sources. In addition, AERMAP determines the receptor height scale relative to surrounding terrain, which directly influences plume behavior and pollutant dispersion patterns [17]. By incorporating detailed elevation data, AERMAP enables AERMOD to account for complex terrain effects, thereby improving the accuracy and reliability of dispersion simulations.

2.2.5 Domain Description and Data Representativeness

As illustrated in Figure 4 and summarized in Table 3, the Khohong meteorological station, located approximately 17 km to the north of study area, and the Sadao meteorological station, situated about 27 km to the south, were selected as representative meteorological data sources for this study. Meteorological data obtained from these stations were used as input parameters for the AERMOD dispersion model. The datasets included wind speed, wind direction, dry-bulb temperature atmospheric pressure, and other variables required for the estimation of atmospheric stability and mixing characteristics.

The modeling domain, as shown in Figure 4, encompassed the emission sources and the surrounding areas potentially affected by pollutant dispersion. The spatial extent of the domain was defined based on the dominant wind directions observed in Songkhla Province. Land-use surface characteristics within the modeling domain were classified as urban for one sector, representing a semi-urban to urban environment characterized by residential areas, commercial activities, and supporting infrastructure. This classification was considered appropriate for the purpose of a pilot-scale assessment.

As the present study was conducted as a preliminary investigation, the effects of building-induced flow disturbances (i.e., building downwash) and background pollutant concentrations were not incorporated into the modeling framework. In addition, wet and dry deposition processes, as well as wet and dry depletion mechanisms, were excluded from the analysis. TSP were therefore treated as non-depositing and non-depleting pollutants throughout the simulation period. This simplified modeling configuration was adopted by primarily evaluating the influence of meteorological conditions on pollutant dispersion and to assess whether the predicted concentration patterns were physically consistent with expected atmospheric transport and diffusion processes.

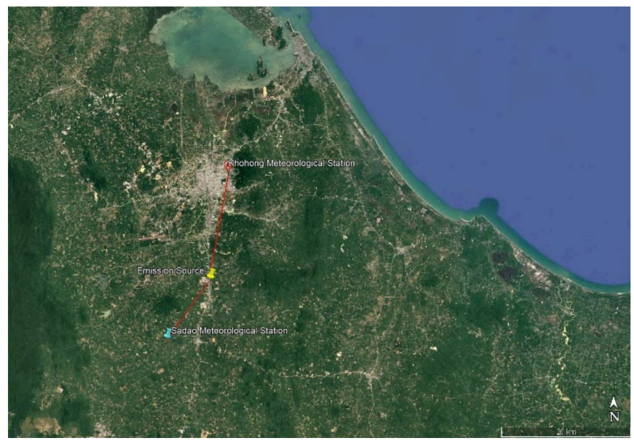

Figure 4 Location of emission source and meteorological stations used in experiment

2.3 Model Evaluation

In this study, 15 receptors were established in four primary directions from the emission sources to evaluate the accuracy and reliability of AERMOD simulations. The model validation process followed the U.S. EPA Protocol for Determining the Best Performing Model (EPA-454/R-92-025), which prescribes the use of both statistical and graphical criteria to assess the degree of agreement between predicted and observed pollutant concentrations.

For AERMOD-simulated TSP concentrations, error-based indicators were first considered. The Mean Absolute Error (MAE) (Eq. 1) measures the average magnitude of deviations between predictions and observations, with lower values indicating better model performance. The Root Mean Square Error (RMSE) (Eq. 2) was also applied; this metric places greater weight on larger discrepancies, meaning that smaller RMSE values reflect improved capability of the model to reproduce observed concentration distributions without substantial deviations. Bias-based indicators were then used to detect systematic tendencies. The Mean Bias Error (MBE) (Eq. 3) quantifies the average signed difference between predictions and observations, where positive values denote overprediction and negative values indicate underprediction. Similarly, the Normalized Mean Bias (NMB) (Eq. 4) expresses bias as a percentage of the observed mean, enabling comparison across receptor sites and pollutants. To assess the temporal representativeness of the model, the Pearson correlation coefficient (R) (Eq. 5) was applied; values approaching 1 denote strong temporal agreement, while values near zero suggest weak or no correlation.

In addition to these measures, the Robust Highest Concentration (RHC) (Eq. 6) was calculated for 24-hour averaging periods. RHC is defined as the meaning of the second through tenth highest ranked concentrations, thereby reducing sensitivity to extreme outliers while still evaluating the model's ability to estimate high-end exposures. Such high-end predictions are particularly important for assessing regulatory compliance and potential health risks. Collectively, these statistical indicators, correlation analyses, and peak concentration metrics provided a comprehensive and objective evaluation of AERMOD performance, as well as the representativeness of meteorological inputs from Khohong and Sadao stations in simulating TSP dispersion.

1. Pearson Correlation Coefficient (R): Measures the strength of the linear relationship between predicted (Pi) and observed (Oi) concentrations. Values close to +1 indicate strong agreement in temporal trends, while values near 0 suggest weak correlation [39][40].

$$R = \frac{\sum_{i=1}^{N}(O_i-\bar{O})(P_i-\bar{P})}{\sqrt{\sum_{i=1}^{N}(O_i-\bar{O})^2}\sqrt{\sum_{i=1}^{N}(P_i-\bar{P})^2}} \quad (1)$$

where O_i is observed value, P_i is the predicted value, $\bar{O}$ is the mean of observed value, $\bar{P}$ is the mean of predicted value, and N is the total number of observations data.

2. Mean Absolute Error (MAE): quantifies the average magnitude of differences between predictions and observations, regardless of direction. A lower MAE indicates closer agreement between simulated and observed TSP concentrations [40][41].

$$MAE = \frac{1}{N}\sum_{i=1}^{N}|P_i - O_i| \quad (2)$$

3. Root Mean Square Error (RMSE): A measure of the spread of prediction errors. It penalizes larger errors more strongly than MAE. Lower RMSE means better agreement [41][42].

$$RMSE = \sqrt{\frac{1}{N}\sum_{i=1}^{N}(P_i - O_i)^2} \quad (3)$$

4. Mean Bias Error (MBE): Reflects whether the model systematically overestimates (positive MBE) or underestimates (negative MBE) compared to observations [41][43].

$$MBE = \frac{1}{N}\sum_{i=1}^{N}(P_i - O_i) \quad (4)$$

5. Normalized Mean Bias (NMB): A normalized form of bias that accounts for the scale of observed concentrations, providing a percentage measure of over- or under-prediction [41][44].

$$NMB = \frac{\sum_{i=1}^{N}(P_i-O_i)}{\sum_{i=1}^{N}O_i} \times 100\% \quad (5)$$

6. Fractional Bias (FB): A symmetric measure of bias that ranges between –2 and +2, with values near zero showing good model performance [41].

$$FB = \frac{2(\bar{P}-\bar{O})}{\bar{P}+\bar{O}} \quad (6)$$

7. Index of agreement (d): A dimensionless statistic that measures how well predictions match observations, with values closer to 1 indicating better agreement [41].

$$d = 1 - \frac{\sum_{i=1}^{N}|P_i-O_i|}{\sum_{i=1}^{N}(|P_i-\bar{O}|+|O_i-\bar{O}|)^2} \quad (7)$$

8. Robust Highest Concentration (RHC): Provides a measure of high-end concentrations by averaging the second through tenth highest 24-hour concentrations. This reduces sensitivity to extreme outliers while retaining the model's ability to represent peak exposure levels [41].

$$RHC = \frac{1}{9}\sum_{j=2}^{10} C_{(j)} \quad (8)$$

where $C_{(j)}$ is the j-th highest ranked 24-hour concentration.

3.0 RESULTS AND DISCUSSION

3.1 Analysis of AERMET-Derived Boundary Layer Parameters

A comparative analysis of AERMET-derived boundary layer parameters (Table 6) indicates that the atmospheric conditions at the Khohong station are more unstable and dispersive than those at the Sadao station, which explains the observed differences in AERMOD-predicted ground-level TSP concentrations. Although the maximum hourly mixing height (Zi) was comparable (2,569 m at Khohong and 2,553 m at Sadao), Khohong exhibited a higher convective frequency (31.68%) than Sadao (26.07%), indicating a greater proportion of convective conditions conducive to pollutant dispersion.

This enhanced instability is further supported by the median Monin-Obukhov length (L), which was less negative at Khohong (-61.10 m) than at Sadao (-74.75 m), indicating stronger surface heat flux and increased turbulence. In addition, the average daytime convective velocity scale (ω*) was higher at Khohong (1.66 m/s) compared to Sadao (1.56 m/s), reflecting more intense vertical mixing. Consequently, the Sadao meteorological profile results in higher localized ground-level TSP concentrations due to weaker vertical dispersion, whereas the enhanced turbulent mixing at Khohong promoted plume dilution over a larger atmospheric volume, leading to lower predicted ground-level impacts under identical emission rates.

Table 6 Quantitative comparison of boundary layer parameters

Parameter	Khohong station	Sadao station
Max hourly mixing height (Zi)	2,569 m	2,553 m
Median Monin-Obukhov length (L)	-61.10 m	-74.75 m
Avg. daytime convective velocity (ω*)	1.66 m/s	1.56 m/s
Convective frequency (%)	31.7	26.1
Stable frequency (%)	8.7	8.0

3.2 Evaluation of AERMOD Simulated Concentrations

The comparative results presented in Table 7 demonstrate that the spatial distribution and magnitude of maximum TSP concentrations simulated by AERMOD varied substantially depending on the meteorological inputs from Khohong and Sadao stations. Although both stations are located within the same regional domain of Southern Thailand, differences in their micrometeorological regimes significantly influenced plume dynamics and surface-level concentration predictions.

Across all averaging periods (1-hour, 24-hour, and annual), simulations driven by Sadao data consistently produced higher maximum concentrations with compact, localized isopleths near the emission source. This pattern reflects weaker wind speeds, higher calm frequencies, and more stable atmospheric stratification associated with Sadao's inland-valley topography, which suppresses vertical mixing and horizontal advection. As a result, pollutants tend to accumulate near the source, particularly under nocturnal and early morning conditions. In contrast, simulations using Khohong data generated broader dispersion patterns, with elongated plumes and lower ground-level gradients, consistent with stronger diurnal winds, greater boundary-layer development, and enhanced turbulent mixing. Variations in wind directionality and frequency between the two stations further shaped receptor exposure footprints, with Sadao indicating higher localized risks and Khohong supporting longer-range transport and dilution.

These findings are consistent with previous studies emphasizing AERMOD's sensitivity to site-specific meteorological inputs [14][26][38]. While both datasets are valid for regulatory applications, their station-specific boundary-layer characteristics produced divergent dispersion outcomes, underscoring the importance of careful station selection. The results also illustrate that identical emission scenarios can yield substantially different exposure profiles depending on meteorological inputs, potentially influencing compliance assessments, health risk evaluations, and policy responses.

Table 7 Compare averaging between Khohong and Sadao meteorological stations

Averaging time	Khohong
1-hour	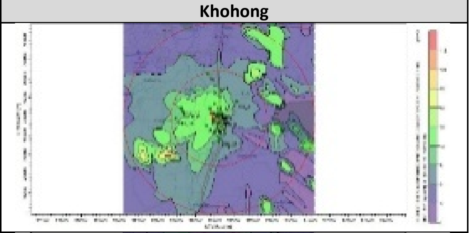
24-hour	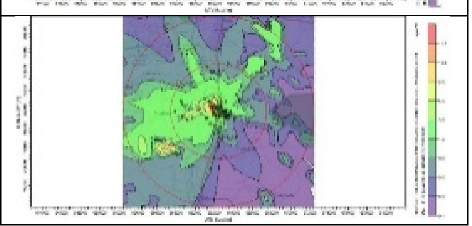
Annual	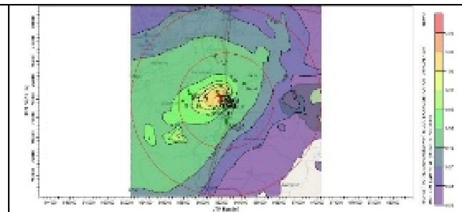
Averaging time	**Sadao**
1-hour	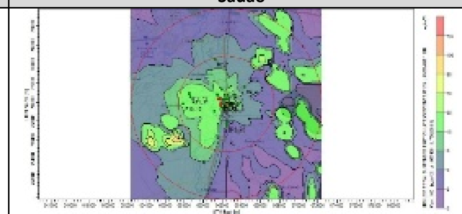
24-hour	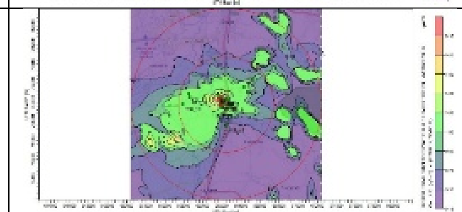
Annual	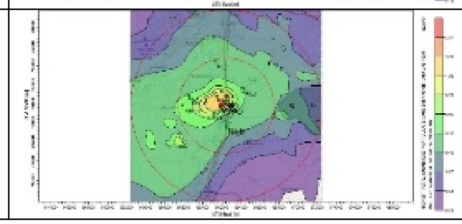

This study contributes new regional evidence by demonstrating, through high-resolution model outputs, how sub-regional meteorological heterogeneity within a 20-km radius can lead to statistically and environmentally significant variations in predicted concentrations. The findings advocate for the incorporation of multiple meteorological datasets in sensitivity analyses and for validating model outputs with observed air quality measurements to identify the most representative station. In contexts where monitoring data are unavailable, the use of both stations in parallel offers a bounded estimate of worst-case and most-likely exposure scenarios, which is particularly important for industrial assessments involving wood-based TSP emissions.

3.2.1 Comparison with The Standard Determined for The 24-Hour and Annual

The maximum predicted concentrations of TSP from the MDF factory during 2020-2023 were evaluated against Thailand's National Ambient Air Quality Standards (NAAQS), which set thresholds of 200 μg/m^3 for 24-hour averages and 80 μg/m^3 for annual averages (Tables 8-9).

Table 8 Thailand national ambient air quality standard

TSP Concentration (μg/m^3)	Averaging Time	Standard
200	24-hour	Thailand NAAQS
80	Annual	

Table 9 Maximum TSP concentration period 2020-2023

Year	Averaging Time	Khohong		Sadao	
		TSP Conc. (μg/m^3)	Location	TSP Conc. (μg/m^3)	Location
2020	1-hour	339.00	657428.19, 756298.88	374.00	657428.19, 756298.88
	24-hour	34.30	657428.19, 756298.88	26.60	661228.19, 760198.88
	Annual	12.10	661328.19, 760098.88	11.90	661128.19, 760198.88
2021	1-hour	102.00	654428.19, 755798.88	118.00	657428.19, 756298.88
	24-hour	8.56	661828.19, 760798.88	11.20	657428.19, 756298.88
	Annual	4.72	661328.19, 760098.88	3.88	661428.19, 759698.88
2022	1-hour	223.00	654428.19, 755798.88	253.00	657428.19, 756298.88
	24-hour	18.50	661828.19, 760798.88	16.80	662028.19, 760298.88
	Annual	6.45	661728.19, 760698.88	8.79	662028.19, 760398.88
2023	1-hour	207.00	657428.19, 756298.88	156.00	654428.19, 755798.88
	24-hour	22.00	657428.19, 756298.88	11.00	662228.19, 759798.88
	Annual	4.22	662028.19, 760098.88	4.91	661928.19, 760398.88

Across all four years, the model results based on both Khohong and Sadao meteorological data indicated that TSP concentrations remained well below the national limits. The highest 24-hour averages ranged from 6.2 to 34.3 μg/m^3, while annual averages varied between 3.9 and 12.1 μg/m^3**.** Although 1-hour maximum concentrations occasionally peaked at values exceeding 300 μg/m^3, these short-term fluctuations did not translate into exceedances of the regulated 24-hour or annual standards.

The results therefore confirm that, under current operating conditions, TSP emissions from the MDF factory do not pose a risk of violating Thailand's ambient air quality regulations. Notably, simulations using Sadao data tended to predict slightly higher localized concentrations than Khohong, but in both cases, the levels remained well within compliance. These findings highlight the consistency of AERMOD predictions across meteorological inputs and reinforce the conclusion that MDF emissions, as modeled, are unlikely to result in sustained air quality exceedances.

3.3 Statistic Methods

3.3.1 Evaluation of Distribution Characteristics Using Q-Q Plots

Quantile-Quantile (Q-Q) plots of the 24-hour average TSP concentrations at 15 receptor locations were used to evaluate the distributional behavior of AERMOD predictions in comparison with observed data. Overall, the simulated concentrations showed good alignment with the 1:1 reference line across the central quantiles, indicating that the model reproduced the general distribution of measured values with acceptable accuracy (Figure 5).

Deviations from the reference line were more evident at the upper quantiles, reflecting the model's reduced ability to capture extreme high-concentration episodes. These discrepancies suggest that while AERMOD can adequately characterize the central tendency of TSP concentrations, caution is needed in interpreting peak values that may influence short-term exposure assessments.

The distribution patterns remained consistent across the four study years (2020-2023), with only minor interannual variability. The stability of the results demonstrates the model's robustness in representing background and typical concentration ranges, while highlighting its limitations in reproducing tail-end extremes. Taken together, the Q-Q analysis confirms that AERMOD is suitable for long-term compliance evaluations but may require complementary approaches or additional calibration when assessing high-impact pollution episodes.

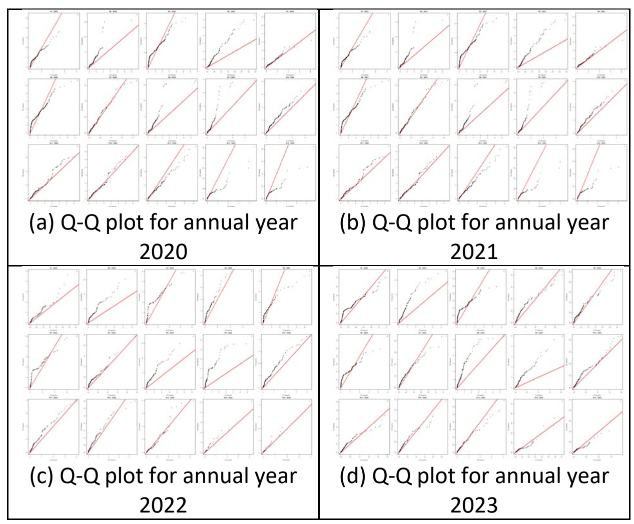

(a) Q-Q plot for annual year 2020
(b) Q-Q plot for annual year 2021
(c) Q-Q plot for annual year 2022
(d) Q-Q plot for annual year 2023

Figure 5 Q-Q plots during period 2020-2023

3.3.2 Evaluation of Distribution Characteristics Using Scatter Plots

Scatter plot matrices were employed to compare observed and modeled 24-hour TSP concentrations using meteorological inputs from Khohong and Sadao stations for the four annual datasets (2020–2023). Each subplot illustrates the relationship between receptor pairs, where points located near the 1:1

reference line indicate closer agreement between model predictions and observations.

In 2020, most receptor sites showed clustering around the reference line, suggesting generally reliable predictions, although some scatter appeared at higher concentrations, reflecting localized overestimation. In 2021, the clustering of mid-range values became more pronounced, indicating slight improvements in model performance, although deviations at extreme values persisted. For 2022, greater variability was observed across receptor sites, with some receptors aligning well with the reference line while others displayed broader scatter, suggesting spatial differences in predictive accuracy within the modeling domain. By 2023, the overall patterns were consistent with earlier years: moderate clustering along the reference line was maintained, but dispersion at higher concentrations remained evident at selected receptors (Figure 6).

Taken together, the scatter plot analysis highlights the moderate agreement between modeled and observed concentrations across multiple years, while also revealing site-specific discrepancies at elevated concentrations. These outcomes confirm that AERMOD captures central tendencies reasonably well under both meteorological inputs but shows limitations in reproducing peak concentration events, particularly in receptor locations strongly influenced by localized meteorological or emission dynamics.

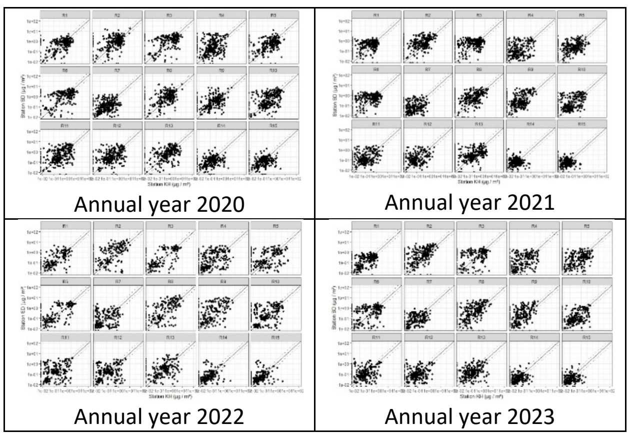

Figure 6 Scatter plots during period 2020-2023

3.3.3 Time Series Plots and Polar Plots

Polar plots generated using meteorological data from Khohong and Sadao stations (Tables 10-11) revealed distinct directional influences on TSP dispersion across the four-year study period. In 2020, higher concentrations were predominantly associated with northeasterly and easterly winds, indicating that emissions from the MDF factory were transported mainly along these pathways. Corresponding time series plots (Tables 12-13) highlighted seasonal variability, with pronounced peaks during the dry season. While sharp short-term spikes were observed, daily averages remained below the NAAQS threshold, with only temporary exceedances recorded.

Table 10 Polar plot (Khohong station) during year 2020-2023

	Khohong
2020	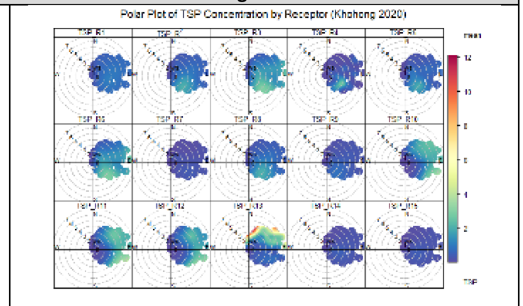
2021	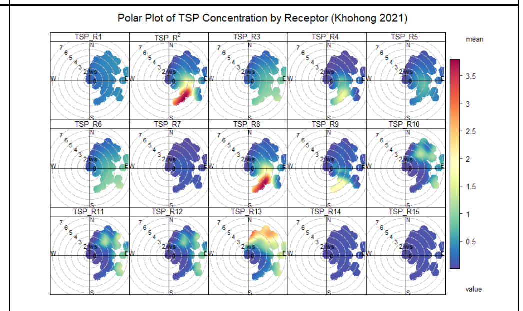
2022	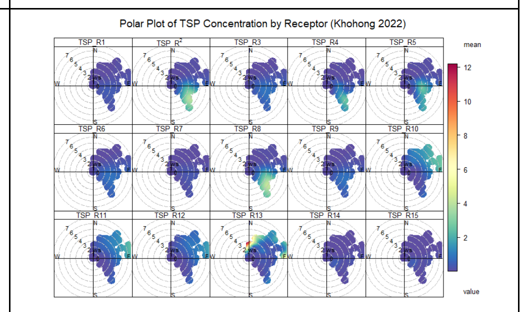
2023	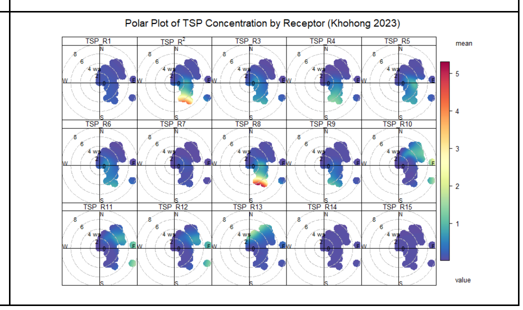

In 2021, the polar plots again emphasized the influence of wind direction, though the intensity of concentration hotspots was slightly reduced compared with 2020. At Khohong, elevated TSP levels were still linked to northeasterly winds, whereas at Sadao they were associated with a broader range of wind sectors. The time series plots indicated episodic exceedances of the 24-hour standard, consistent with the previous year, but overall concentration complied with the annual NAAQS limit. By 2022, the polar plots displayed more dispersed concentration patterns, with multiple wind sectors contributing to elevated TSP levels. This dispersion suggests increased variability in atmospheric transport conditions influencing pollutants spread from the factory. Time series plots for the same year revealed more frequent short-term peaks compared to earlier years, including several exceedances of the 24-hour standard at certain receptors, although annual averages still complied with national regulations.

In 2023, polar plots showed patterns like previous years, with elevated concentrations aligned to prevailing northeasterly and easterly winds at Khohong, and across broader sectors at Sadao. Time series data demonstrated repeated short-term spikes, some exceeding the 24-hour limit. Despite the frequency of exceedances, the annual averages remained below the national standard, suggesting that emissions from the MDF factory contributed primarily to episodic rather than sustained impacts on local air quality.

Table 11 Polar plot (Sadao station) during year 2020-2023

Sadao	
2020	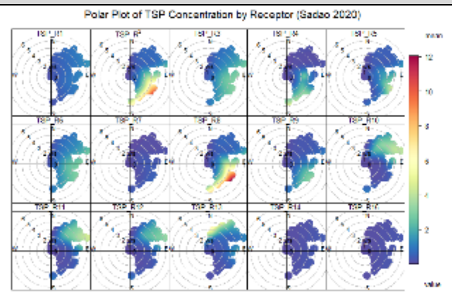
2021	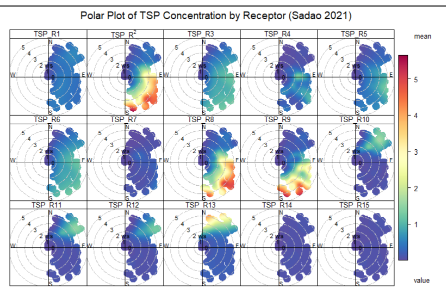
2022	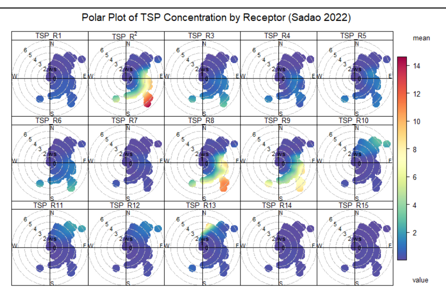
2023	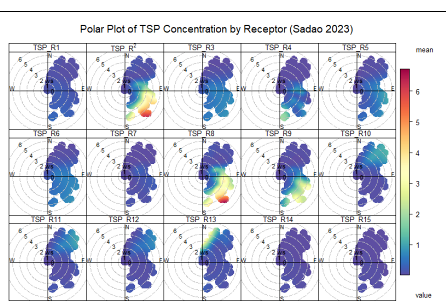

Table 12 Time series plot (Khohong station) during year 2020-2023

Khohong	
2020	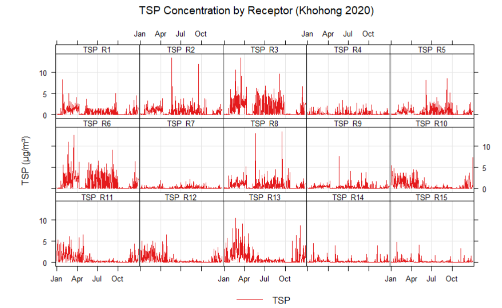
2021	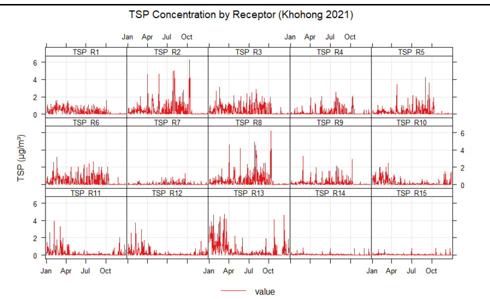
2022	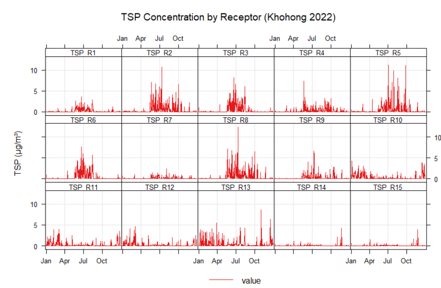
2023	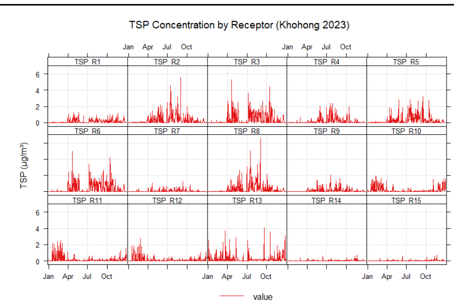

3.4 Evaluation of Model Validation Using Statistical Methods

Model validation was conducted over the four-year period (2020-2023) using a suite of statistical indicators (Eq. 1-8) to assess the performance of AERMOD with meteorological inputs from Khohong and Sadao stations (Tables 14-17). The correlation coefficient (R) demonstrated substantial variability across receptors and years, ranging from weak (<0.2) to moderate (0.5-0.6), indicating that while AERMOD was able to capture general temporal trends, receptor-specific factors and meteorological variability limited its consistency. Error-based metrics, including MAE and RMSE, highlighted higher inaccuracies at receptors closer to or directly downwind of the emission source, reflecting the challenges of simulating near-source dispersion and localized turbulence.

Table 13 Time series plot (Sadao station) during year 2020- 2023

	Sadao
2020	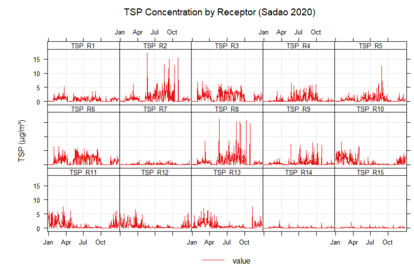
2021	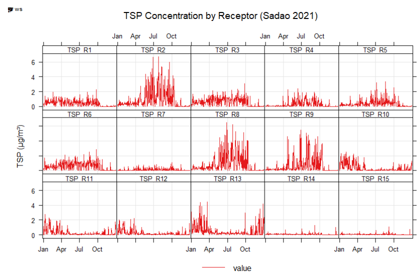
2022	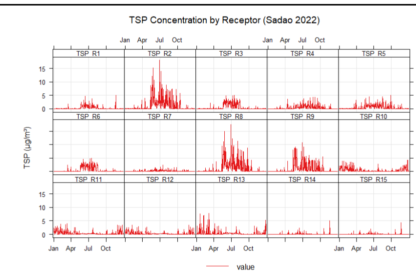
2023	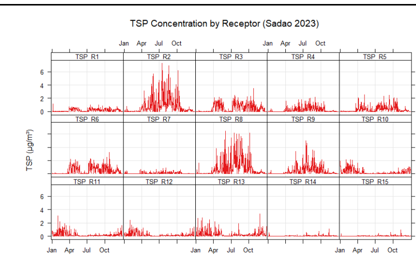

Bias-related indicators such as MBE and NMB revealed alternating patterns of overestimation and underestimation across years. Positive bias values were more common in 2020 and 2021, whereas a mix of positive and negative values appeared in 2022 and 2023, suggesting that prediction accuracy varied with receptor placement and interannual changes in atmospheric conditions. FB values generally remained within the ±0.67 acceptance range, though some receptors exceeded this threshold, pointing to localized systematic deviations. The Index of Agreement (d) ranged between 0.4 and 0.7, reflecting moderate skill but not uniformly strong performance across sites and years.

Further insights were provided by the Robust Highest Concentration (RHC), particularly relevant for regulatory compliance with 24-hour standards. In 2020 and 2021, RHC values derived from Sadao station were often higher than those from Khohong, consistent with its closer proximity to the source and its ability to represent local meteorological influences. In contrast, by 2022, several receptors showed higher RHCs under Khohong inputs, reflecting interannual differences in wind regimes and boundary-layer dynamics. By 2023, Sadao again yielded relatively higher RHC values at key receptors, although convergence between the two datasets was observed at some sites.

Overall, the four-year validation underscores the sensitivity of AERMOD outputs to meteorological inputs under tropical monsoon conditions. Sadao data tended to capture higher localized concentrations and may be more representative of near-source dispersion, whereas Khohong data produced smoother, regionally averaged results. The consistent but imperfect performance across statistical indicators suggests that AERMOD provides a reasonably robust tool for assessing TSP impacts from MDF emissions, while highlighting uncertainties linked to meteorological variability and receptor-specific conditions. These findings emphasize the importance of employing multi-station meteorological evaluations, robust statistical validation, and cautious interpretation of high-concentration events when applying AERMOD for regulatory or health risk assessments in complex tropical environments.

Table 14 Model validation during period 2020

Receptor	R	MAE	RMSE	MBE	NMB	FB	d	RHC	
								Khohong	Sadao
R1	0.349	0.557	0.958	0.001	0.002	0.002	0.582	8.004	5.177
R2	0.351	1.063	2.164	0.590	0.788	0.565	0.515	13.325	17.160
R3	0.452	1.202	1.943	0.052	0.036	0.035	0.673	13.290	7.163
R4	0.210	0.642	1.261	0.377	1.289	0.784	0.346	3.450	6.559
R5	0.220	0.696	1.320	0.112	0.176	0.162	0.447	8.572	11.985
R6	0.443	1.142	1.859	0.041	0.030	0.029	0.663	12.565	6.578
R7	0.127	0.221	0.392	0.013	0.067	0.065	0.388	2.153	1.639
R8	0.297	1.115	2.377	0.619	0.837	0.590	0.461	13.422	16.199
R9	0.347	0.497	1.131	0.256	0.753	0.547	0.488	7.273	7.779
R10	0.435	0.803	1.375	0.254	0.354	0.301	0.637	7.208	7.990
R11	0.336	0.794	1.478	0.126	0.175	0.161	0.566	6.480	7.455
R12	0.297	0.659	1.251	0.050	0.083	0.079	0.538	6.403	6.530
R13	0.288	0.921	1.735	0.183	0.176	0.193	0.509	10.376	7.577
R14	0.042	0.213	0.539	0.073	0.326	0.389	0.236	4.485	2.501
R15	0.052	0.196	0.503	0.075	0.361	0.440	0.236	4.643	2.033

Table 15 Model validation during period 2021

Receptor	R	MAE	RMSE	MBE	NMB	FB	d	RHC	
								Khohong	Sadao
R1	0.276	0.324	0.477	0.128	0.428	0.353	0.548	1.585	2.239
R2	0.406	0.689	1.256	0.449	0.990	0.662	0.566	6.197	6.691
R3	0.267	0.507	0.726	0.201	0.469	0.380	0.547	3.096	3.027
R4	0.308	0.270	0.498	0.078	0.405	0.337	0.545	2.529	2.411
R5	0.223	0.349	0.625	0.117	0.448	0.366	0.450	4.195	3.354
R6	0.264	0.486	0.699	0.189	0.460	0.374	0.542	3.138	2.831
R7	0.135	0.131	0.227	0.032	0.380	0.319	0.386	1.262	1.072
R8	0.400	0.663	1.223	0.428	0.972	0.654	0.564	6.115	6.466
R9	0.491	0.501	1.025	0.425	2.202	1.048	0.473	3.270	5.461
R10	0.424	0.292	0.520	0.116	0.520	0.413	0.615	2.453	2.502
R11	0.312	0.279	0.527	0.075	0.368	0.311	0.526	3.844	2.721
R12	0.290	0.234	0.456	0.051	0.297	0.259	0.502	3.677	2.201
R13	0.228	0.561	1.021	0.044	0.082	0.086	0.470	4.761	4.475
R14	0.041	0.072	0.157	0.016	0.285	0.249	0.142	0.832	1.232
R15	0.031	0.063	0.138	0.012	0.230	0.206	0.157	0.789	1.082

Table 16 Model validation during period 2022

Receptor	R	MAE	RMSE	MBE	NMB	FB	d	RHC	
								Khohong	Sadao
R1	0.424	0.239	0.609	0.082	0.417	0.345	0.599	3.525	4.946
R2	0.529	1.062	2.328	0.772	1.493	0.855	0.588	10.528	17.789
R3	0.599	0.404	0.954	0.108	0.254	0.225	0.761	8.113	4.996
R4	0.194	0.468	0.940	0.138	0.490	0.394	0.409	7.125	4.370
R5	0.251	0.605	1.419	0.037	0.073	0.076	0.445	11.221	4.928
R6	0.593	0.395	0.915	0.107	0.260	0.230	0.757	7.478	4.980
R7	0.151	0.199	0.396	0.049	0.381	0.320	0.394	2.336	2.378
R8	0.512	1.043	2.303	0.726	1.338	0.802	0.594	12.095	17.256
R9	0.416	0.799	1.828	0.664	2.719	1.152	0.424	6.545	10.698
R10	0.309	0.518	0.929	0.173	0.504	0.403	0.541	4.238	4.269
R11	0.333	0.433	0.793	0.119	0.405	0.337	0.575	4.030	3.924
R12	0.297	0.358	0.685	0.076	0.303	0.263	0.549	4.560	3.509
R13	0.244	0.575	1.291	0.004	0.008	0.008	0.463	8.422	7.862
R14	0.025	0.124	0.459	0.027	0.338	0.289	0.126	4.027	4.894
R15	0.014	0.109	0.405	0.017	0.239	0.213	0.115	3.709	4.141

Table 17 Model validation during period 2023

Receptor	R	MAE	RMSE	MBE	NMB	FB	d	RHC	
								Khohong	Sadao
R1	0.325	0.174	0.275	0.039	0.250	0.222	0.582	1.230	1.126
R2	0.563	0.615	1.167	0.476	1.483	0.852	0.604	5.485	7.226
R3	0.382	0.455	0.769	0.082	0.196	0.178	0.625	5.226	3.422
R4	0.265	0.258	0.486	0.060	0.326	0.280	0.494	2.375	2.151
R5	0.312	0.317	0.571	0.035	0.128	0.120	0.542	3.213	2.524
R6	0.378	0.433	0.732	0.075	0.189	0.172	0.620	4.912	3.211
R7	0.255	0.109	0.195	0.010	0.111	0.105	0.501	1.269	0.878
R8	0.504	0.649	1.230	0.490	1.476	0.849	0.580	6.439	6.414
R9	0.507	0.353	0.698	0.285	2.163	1.039	0.479	2.031	4.959
R10	0.330	0.250	0.455	0.058	0.285	0.250	0.572	1.961	2.155
R11	0.281	0.229	0.451	0.043	0.246	0.219	0.524	2.500	2.985
R12	0.291	0.192	0.375	0.030	0.200	0.182	0.531	2.688	2.371
R13	0.114	0.335	0.688	0.006	0.023	0.023	0.372	4.064	3.329
R14	0.162	0.051	0.109	0.005	0.112	0.106	0.368	0.699	1.031
R15	0.120	0.046	0.101	0.001	0.034	0.033	0.316	0.734	0.945

4.0 CONCLUSION

This study presents a four-year evaluation (2020-2023) of AERMOD simulations to assess the TSP dispersion emitted from the MDF manufacturing industry in Southern Thailand, with particular emphasis on the influence of site-specific meteorological data. The results clearly demonstrate that meteorological inputs play a decisive role in determining the magnitude and spatial distribution of predicted ground-level concentrations. Quantitative comparisons of AERMET-derived boundary layer parameters reveal distinct atmospheric regimes between the two representative meteorological stations. The Khohong station exhibited a higher maximum hourly mixing height (Zi) of 2,569 m and a substantially greater convective frequency of 31.7%, compared with 2,553 m and 26.1%, respectively, at the Sadao station.

In addition, the median Monin-Obukhov length (L) was less negative at Khohong (-61.1 m) than at Sadao (-74.8 m), indicating a more unstable surface layer and enhanced vertical turbulent mixing at Khohong. These boundary layer characteristics explain the higher localized ground-level TSP concentrations predicted when using Sadao meteorological data, which are associated with weaker winds and more frequent stable stratification. In contrast, the more unstable and convective conditions represented by the Khohong data promote wider plume dispersion and consequently lower predicted ground-level impacts under identical emission scenarios.

Despite these inter-station differences, all predicted 24-hour and annual average TSP concentrations remained below Thailand's National Ambient Air Quality Standards of 200 µg/m³ and 80 µg/m³, respectively. Although short-term episodic concentration peaks were occasionally observed, annual average concentration consistently complied with the applicable regulatory limits, suggesting that emissions from the MDF industry are unlikely to result in sustained exceedances of ambient air quality standards.

Overall, the findings underscore the critical importance of meteorological station selection and the associated boundary layer parameters-particularly mixing height and convective frequency-in influencing AERMOD simulation outcomes under tropical monsoon conditions. The incorporation of meteorological data from multiple representative stations is therefore recommended to better capture localized atmospheric variability and to support more robust air quality assessment, management strategies, and evidence-based policy decisions.

Acknowledgement

Authors wish to express their sincere appreciation to all individuals and organizations that contributed to the successful completion of this study. Special appreciation is extended to the staff of the Department of Civil and Environmental Engineering, Faculty of Engineering, the Graduate school and the Air Pollution and Health Effect Research Center, Prince of Songkla University, for their valuable assistance in providing essential data and technical support.

Conflicts of Interest

The author(s) declare(s) that there is no conflict of interest regarding the publication of this paper

References

[1] Priha, E., S. Pennanen, T. Rantio, J. Uitti, and J. Liesivuori. 2004. Exposure to and acute effects of medium-density fiber board dust. *Journal of Occupational and Environmental Hygiene.* 1(11): 738–744. DOI: https://doi.org/10.1080/15459620490520774

[2] Chung, K. Y., R. J. Cuthbert, G. S. Revell, S. G. Wassel, and N. Summers. 2000. A study on dust emission, particle size distribution and formaldehyde concentration during machining of medium density fibreboard. *The Annals of Occupational Hygiene.* 44(6): 455–466. DOI: https://doi.org/10.1093/annhyg/44.6.455

[3] Ding, T., J. Zhao, N. Zhu, and C. Wang. 2020. A comparative study of morphological characteristics of medium-density fiberboard dust by sieve and image analyses. *Journal of Wood Science.* 66: 18. DOI: https://doi.org/10.1186/s10086-020-01896-x

[4] Hiziroglu, S., and P. Kosonkorn. 2006. Evaluation of surface roughness of Thai medium density fiberboard (MDF). *Building and Environment.* 41: 527–533. DOI: https://doi.org/10.1016/j.buildenv.2005.02.016

[5] U.S. Environmental Protection Agency (EPA). 2002. AP-42 Compilation of Air Pollutant Emission Factors: Chapter 10.6.1 – Medium Density Fiberboard (MDF) Manufacturing. https://www.epa.gov/air-emissions-factors-and-quantification/ap-42-compilation-air-emissions-factors Retrieved on 15 January 2025

[6] Thetkathuek, A., T. Yingratanasuk, and W. Ekburanawat. 2016. Respiratory symptoms due to occupational exposure to formaldehyde and MDF dust in a MDF furniture factory in Eastern Thailand*. Advances in Preventive Medicine.* 2016: 3705824. DOI: https://doi.org/10.1155/2016/3705824

[7] Cui, Y., J. Yin, Y. Cai, H. Wang, N. Zhu, and T. Ding. 2022. Spatial distribution characteristics of the dust emitted at different cutting speeds during MDF milling by image analysis. *Journal of Wood Science.* 68(1): 17. DOI: https://doi.org/10.1186/s10086-022-02025-6

[8] Thetkathuek, A., T. Yingratanasuk, W. Ekburanawat, W. Jaidee, and T. Sa-ngiamsak. 2020. The risk factors for occupational contact dermatitis among workers in a medium density fiberboard furniture factory in Eastern Thailand. *Archives of Environmental & Occupational Health.* 75(6): 1–11. https://doi.org/10.1080/19338244.2020.1819185

[9] Thetkathuek, A., T. Yingratanasuk, and W. Ekburanawat. 2016. Respiratory symptoms due to occupational exposure to formaldehyde and MDF dust in a MDF furniture factory in Eastern Thailand. *Advances in Preventive Medicine.* 2016: 3705824. https://doi.org/10.1155/2016/3705824

[10] Occupational Safety and Health Administration (OSHA). 2025. Wood dust – Hazards. https://www.osha.gov/wood-dust/hazards Retrieved on 15 June 2025

[11] Suriyawong, P., S. Chuetor, H. Samae, S. Piriyakarnsakul, M. Amin, M. Furuuchi, M. Hata, M. Inerb, and W. Phairuang. 2023. Airborne particulate matter from biomass burning in Thailand: Recent issues, challenges, and options. *Heliyon.* 9(3): e14261. DOI: https://doi.org/10.1016/j.heliyon.2023.e14261

[12] Pollution Control Department (PCD). 2022. Thailand State of Pollution Report 2022. Ministry of Natural Resources and Environment. https://www.pcd.go.th/wp-content/uploads/2022/08/pcdnew-2022-08-08_08-30-05_795080.pdf Retrieved on30 January 2025

[13] Cimorelli, A. J., S. G. Perry, A. Venkatram, J. C. Weil, R. J. Paine, R. B. Wilson, and R. F. Lee. 2005. AERMOD: A dispersion model for industrial source applications. Part I: General model formulation and boundary layer characterization*. Journal of Applied Meteorology*. 44(5): 682–693. DOI: https://doi.org/10.1175/JAM2227.1

[14] Perry, S. G., A. J. Cimorelli, R. J. Paine, R. W. Brode, J. C. Weil, A. Venkatram, and R. B. Wilson. 2005. AERMOD: A dispersion model for industrial source applications. Part II: Model performance against 17 field study databases. *Journal of Applied Meteorolog*y. 44(5): 694–708. DOI: https://doi.org/10.1175/JAM2228.1

[15] U.S. Environmental Protection Agency (EPA). 2019. AERMOD Modeling System Overview. https://www.epa.gov/scram/air-quality-dispersion-

modeling-preferred-and-recommended-models#aermod Retrieved on30 January 2025

[16] U.S. Environmental Protection Agency (EPA). 2024a. User's Guide for the AMS/EPA Regulatory Model – AERMOD. https://gaftp.epa.gov/Air/aqmg/SCRAM/models/preferred/aermod/aermod_userguide.pdf Retrieved on15 January 2025

[17] U.S. Environmental Protection Agency (EPA). 2024b. AERMOD Model Evaluation. EPA-454/B-24-006. https://nepis.epa.gov/Exe/ZyPDF.cgi/P101CGTM.PDF?Dockey=P101CGTM.PDF Retrieved on30 January 2025

[18] U.S. Environmental Protection Agency (EPA). 2024c. AERMOD Model Formulation. EPA-454/B-24-010. https://nepis.epa.gov/Exe/ZyPDF.cgi/P101CLHZ.PDF?Dockey=P101CLHZ.PDF Retrieved on30 January 2025

[19] Fadavi, A., M. F. Abari, and M. A. Nadoushan. 2016. Evaluation of AERMOD for distribution modeling of particulate matters (Case study: Ardestan Cement Factory). *International Journal of Pharmaceutical Research & Allied Sciences.* 5(4): 262–270.

[20] Jayadipraja, E. A., A. Daud, M. A. H. Assegaf, and M. Maming. 2017. The application of the AERMOD model in the environmental health to identify the dispersion area of total suspended particulate from cement industry stacks. *International Journal of Research in Medical Sciences.* 4(6): 2044–2049. DOI: https://doi.org/10.18203/2320-6012.ijrms20161757

[21] Zou, B., F. B. Zhan, J. T. Wilson, and Y. Zeng. 2010. Performance of AERMOD at different time scales. *Simulation Modelling Practice and Theory.* 18: 612–623. DOI: https://doi.org/10.1016/j.simpat.2010.01.005

[22] Kakosimos, K. E., M. J. Assael, and A. S. Katsarou. 2011. Application and evaluation of AERMOD on the assessment of particulate matter pollution caused by industrial activities in the Greater Thessaloniki area. *Environmental Technology.* 32(6): 593–608. DOI: https://doi.org/10.1080/09593330.2010.506491

[23] Khamyingkert, L., and S. Thepanondh. 2016. Analysis of industrial source contribution to ambient air concentration using AERMOD dispersion model. *EnvironmentAsia.* 9(1): 28–36. DOI: https://doi.org/10.14456/ea.2016.4

[24] Kesarkar, A. P., M. Dalvi, A. Kaginalkar, and A. Ojha. 2007. Coupling of the weather research and forecasting model with AERMOD for pollutant dispersion modeling. *Atmospheric Environmen*t. 41(9): 1976–1988. DOI: https://doi.org/10.1016/j.atmosenv.2006.10.042

[25] Kumar, A., S. Dixit, C. Varadarajan, A. Vijayan, and A. Masuraha. 2006. Evaluation of the AERMOD dispersion model as a function of atmospheric stability for an urban area. *Environmental Progress.* 25(2): 141–151. DOI: https://doi.org/10.1002/ep.10129

[26] Kumar, A., R. S. Patil, A. K. Dikshit, R. Kumar, J. Brandt, and O. Hertel. 2016. Assessment of impact of unaccounted emission on ambient concentration using DEHM and AERMOD in combination with WRF. *Atmospheric Environment.* 142: 406–413. DOI: https://doi.org/10.1016/j.atmosenv.2016.08.024

[27] Kumar, A., R. S. Patil, A. K. Dikshit, and R. Kumar. 2017. Application of WRF model for air quality modelling and AERMOD – A survey. *Aerosol and Air Quality Research.* 17: 1925–1937. DOI: https://doi.org/10.4209/aaqr.2016.06.0265

[28] Chusai, C., K. Manomaiphiboon, P. Saiyasitpanich, and S. Thepanondh. 2012. NO_2 and SO_2 dispersion modeling and relative roles of emission sources over Map Ta Phut industrial area, Thailand. *Journal of the Air & Waste Management Association.* 62(8): 932–945. DOI: https://doi.org/10.1080/10962247.2012.687704

[29] Thawonkaew, A., S. Thepanondh, D. Sirithian, and L. Jinawa. 2021. Assimilative capacity of air pollutants in an area of the largest petrochemical complex in Thailand. *GEOMATE Journal*. 11(23): 2162–2169. DOI: https://doi.org/10.21660/2021.76.2517

[30] Loo, Y. Y., L. Billa, and A. Singh. 2015. Effect of climate change on seasonal monsoon in Asia and its impact on the variability of monsoon rainfall in Southeast Asia. *Geoscience Frontiers.* 6(6): 817–823. DOI: https://doi.org/10.1016/j.gsf.2014.02.009

[31] Thai Meteorological Department (TMD). 2023. Climatological Reports and Monsoon Data for Southern Thailand. https://www.tmd.go.th Retrieved on15 October 2023

[32] Durre, I., R. S. Vose, and D. B. Wuertz. 2006. Overview of the Integrated Global Radiosonde Archive. *Journal of Climate.* 19(1): 53–68. DOI: https://doi.org/10.1175/JCLI3594.1

[33] Malakan, W., J. Keawboonchu, and S. Thepanondh. 2018. Comparison of AERMOD performance using observed and prognostic meteorological data. EnvironmentAsia. 11(2): 38–52. https://doi.org/10.14456/ea.2018.21

[34] Amatayakul, P., and T. Chomtha. 2013. Agricultural Meteorology to Know for Songkhla. *Meteorological Department*. 551.6593.17-2013

[35] Eastern Economic Corridor Office. 2020. Environmental Guidelines for Air Quality Modeling in EIA Reports. https://www.eeco.or.th/en Retrieved on 20 January 2025

[36] Hanna, S. R., and J. Chang. 2012. Acceptance criteria for urban dispersion model evaluation. *Meteorology and Atmospheric Physics*. 116: 133–146. DOI: https://doi.org/10.1007/s00703-011-0177-1

[37] U.S. Environmental Protection Agency (EPA). 2024d. User's Guide for the AERMOD Terrain Preprocessor (AERMAP). EPA-454/B-24-008. https://nepis.epa.gov/Exe/ZyPDF.cgi/P101D4C5.PDF?Dockey=P101D4C5.PDF Retrieved on 15 January 2025

[38] U.S. Environmental Protection Agency (EPA). 2024e. User's Guide for the AERMOD Meteorological Preprocessor (AERMET). EPA-454/B-24-004. https://gaftp.epa.gov/Air/aqmg/SCRAM/models/met/aermet/aermet_userguide.pdf

[39] Willmott, C. J. 1982. Some comments on the evaluation of model performance. *Bulletin of the American Meteorological Society.* 63: 1309–1313. DOI: https://doi.org/10.1175/1520-0477

[40] Willmott, C. J., and K. Matsuura. 2005. Advantages of the mean absolute error (MAE) over the root mean square error (RMSE) in assessing average model performance. Climate Research. 30: 79–82. DOI: https://doi.org/10.3354/cr030079

[41] U.S. Environmental Protection Agency (EPA). 1992. *Protocol for Determining the Best Performing Model.* EPA-454/R-92-025. https://www.epa.gov/sites/default/files/2020- Retrieved on30 January 202510/documents/model_eval_protocol.pd Retrieved on 15 January 2025

[42] Hanna, S. R. 1989. Confidence limits for air quality model evaluations, as estimated by bootstrap and jackknife resampling methods. *Atmospheric Environment.* 23(6): 1385–1398. DOI: https://doi.org/10.1016/0004-6981(89)90162-9

[43] Chang, J. C., and S. R. Hanna. 2004. Air quality model performance evaluation. *Meteorology and Atmospheric Physics*. 87(1–3): 167–196. DOI: https://doi.org/10.1007/s00703-003-0070-7

[44] Boylan, J. W., and A. G. Russell. 2006. PM and light extinction model performance metrics, goals, and criteria for three-dimensional air quality models. *Atmospheric Environment.* 40(26): 4946-4959. DOI: https://doi.org/10.1016/j.atmosenv.2005.09.087